International Conference on Space Optics—ICSO 2004

Toulouse, France

30 March–2 April 2004

Edited by Josiane Costeraste and Errico Armandillo

IASI instrument: technical description and measured performances

Ph. Hébert, D. Blumstein, C. Buil, T. Carlier, et al.

International Conference on Space Optics — ICSO 2004, edited by Errico Armandillo, Josiane Costeraste, Proc. of SPIE Vol. 10568, 1056806 · © 2004 ESA and CNES
CCC code: 0277-786X/17/$18 · doi: 10.1117/12.2308007

IASI INSTRUMENT : TECHNICAL DESCRIPTION AND MEASURED PERFORMANCES

Ph. Hébert[(1)], D. Blumstein[(1)], C. Buil[(1)], T. Carlier[(1)], G. Chalon[(1)]
P. Astruc[(2)], A. Clauss[(2)], D. Siméoni[(2)]
B. Tournier[(3)]

[(1)]CNES, 18 avenue Edouard Belin – 31401 Toulouse Cedex 9 – France
[(2)]Alcalel Cannes – 100 boulevard du Midi BP 99 – 06156 Cannes la Bocca Cedex – France
[(3)]Noveltis – Parc Technologique du Canal – 2, av. de l'Europe – 31526 Ramonville St Agne Cedex - France

ABSTRACT

IASI is an infrared atmospheric sounder. It will provide meteorologist and scientific community with atmospheric spectra. The IASI system includes 3 instruments that will be mounted on the Metop satellite series, a data processing software integrated in the EPS (EUMETSAT Polar System) ground segment and a technical expertise centre implemented in CNES Toulouse.
The instrument is composed of a Fourier transform spectrometer and an associated infrared imager. The optical configuration is based on a Michelson interferometer and the interferograms are processed by an on-board digital processing subsystem, which performs the inverse Fourier transforms and the radiometric calibration. The infrared imager co-registers the IASI soundings with AVHRR imager (AVHRR is another instrument on the Metop satellite).
The presentation will focus on the architectures of the instrument, the description of the implemented technologies and the measured performance of the first flight model.
CNES is leading the IASI program in association with EUMETSAT. The instrument Prime is ALCATEL SPACE

1. IASI PROGRAMME

IASI (Infrared Atmospheric Sounding Interferometer) is a key element of the payload on the Metop series of European meteorological polar-orbiting satellites. The first flight model in this series is scheduled for launch in 2005. IASI is a significant technological and scientific step forward that will provide meteorologists with atmospheric emission spectra to derive temperature and humidity [1].
The instrument is designed to measure atmospheric spectra in the infrared. It comprises a Fourier transform spectrometer and an associated imager [2].
CNES led the IASI project as prime contractor up to the end of the preliminary definition phase.
The instrument development phase started in November 1998. This phase and production of recurring models are being led by Alcatel Space as industrial prime contractor. The corresponding contract covers the supply of three flight models, with delivery of the first model in 2003.
For the IASI program a cooperation agreement has been approved by CNES and EUMETSAT. Under this agreement, CNES has technical oversight responsibility for the instruments development, and will develop the data processing software and operate a technical expertise centre. EUMETSAT is responsible for operating IASI, archiving and distribution of the data to users.

2. IASI OBJECTIVES AND METEOROLOGICAL CONSTRAINTS

2.1 Scientific objectives

The levels of accuracy required for numerical weather forecast or data assimilation systems are :
- 1 K absolute accuracy and 1 km vertical resolution for temperature profiles;
- 10% relative accuracy and 1 km vertical resolution for humidity profiles.

In areas of clear sky or partly cloudy sky, global coverage of the sounding system will be ensured by the simultaneous use of the microwave sounders AMSU-A and MHS.

IASI must also be able to measure the contents of O_3, CH_2, CO and N_2O gas constituents. The accuracy expected is over 5% for ozone measurement (and whenever possible, a description of the profile at 2 or 3 levels) and over 10% for other gases.

IASI must be able to determine ocean and continent surface temperatures.

Finally, IASI must contribute to the study of clouds in terms of part coverage, cloud top temperature, type and transparency; and cloud optical property variations with the wavelength.

The definition of measurement objectives is supplemented by the description of the temporal and horizontal resolutions expected, i.e. 12 hours (lapse of time between two successive satellite crossings) and 25 km at sub-satellite point.

2.2 Spectral characteristics

The operable spectral range extends from the end of the atmospheric transmission window at 3.62µm (2 760 cm^{-1}) to beyond the Q branch peak of the CO_2 absorption band, circa 15.5µm (645 cm^{-1}).

The spectral resolution specification results from the line spacing within the CO_2 absorption band at 15µm, i.e. 1.5 cm^{-1}. The spectral resolution required from IASI after apodisation is equal to 0.5 cm^{-1}, which is derived, before apodisation, as :

Table 1. Specification of non-apodised spectral resolution

ν (cm^{-1})	$\Delta\nu$ (cm^{-1})
645	0.35
1210	0.35
2000	0.39
2450	0.45
2760	0.50

Knowledge of the IASI spectral response function must be of a quality such that the error induced on the determination of an atmospheric target temperature will be less than 0.1 K. This leads to the notion of shape error index ε. It is the area of the difference calculated in [-16 cm^{-1} : +16 cm^{-1}] between the real part of the **actual** Instrument Line Shape (ILS) and the real part of a **reference** ILS. ε is divided in ε_1 and ε_2. ε_2 includes the effects of microvibrations, ε_1 deals with all other effects. These parameters are specified in table 2 :

Table 2. Specification of shape error index

ν band (cm^{-1})	ε_1	ε_2
[645 : 1210]	= 0.02	= 0.026
[1210 : 2000]	= 0.03	= 0.026
[2000 : 2450]	= 0.04	= 0.03
[2450 : 2760]	= 0.05	= 0.042

Finally, in terms of instrument wave number calibration, the central wave number of each channel must be measured with a relative accuracy higher than 2.10^{-6}. At the instrument level, it means that the ILS centroïd should have a relative stability of 10^{-6} after calibration, and accuracy of the prediction before the spectral calibration performed on ground of 2.10^{-4} (relative).

2.3 Radiance measurement characteristics

2.3.1 Sensitivity

The instrument radiometric sensitivity is defined as the temperature variation which gives a black body radiance variation equivalent to the measurement's noise. Its evaluation in terms of radiance depends on the wave number and the temperature. For reasons of convenience, this temperature is specified independently from the channel and the reference temperature adopted is 280 K. The specified radiometric sensitivity ranges from 0.2 K at 650 cm^{-1} to 0.36 K at 2700 cm^{-1}, in the mission spectral bands. The noise taken into account by this specification includes all noise sources (detectors, amplifiers, digitizing, processing) and errors considered as noise (e.g. errors linked to wave number calibration or instrument function knowledge).

2.3.2 Calibration

For target temperature between 200 K and 300 K :
(a) The accuracy (maximum absolute error) in temperature determination should be better than 0.5 K at 280 K.
(b) Calibration reproducibility must be less than 0.3 K.
(c) Inter-band, inter-pixel and along the track calibration variations must not be higher than 0.2 K.
Finally, as far as the temperature range is concerned, IASI must be able to measure equivalent temperatures from 4 K to 315 K.

2.4 Geometrical characteristics

The IASI scanning is compatible with that of the AMSU-A sounder : it stares at the same ground positions during scanning. More precisely, the IASI optical axis scans the space in a plane which is perpendicular to the satellite orbit track (Fig. 1). The scanning process is step by step, with rapid move between the different look positions, and a stop during the look (acquisition of interferogram). There are 30 look positions on the measurement track, spaced by approximately 3.3 degrees, from -47.85 degrees to +47.85 degrees with respect to the nadir. In addition to the 30 views in the ground direction, the scanning includes views to the calibration targets and return to the starting position; overall, it lasts 8 seconds. Bearing in mind that METOP will be in orbit at an altitude close to 840 km, the IASI swath (length of ground measurement track) will be approximately 2400 km.

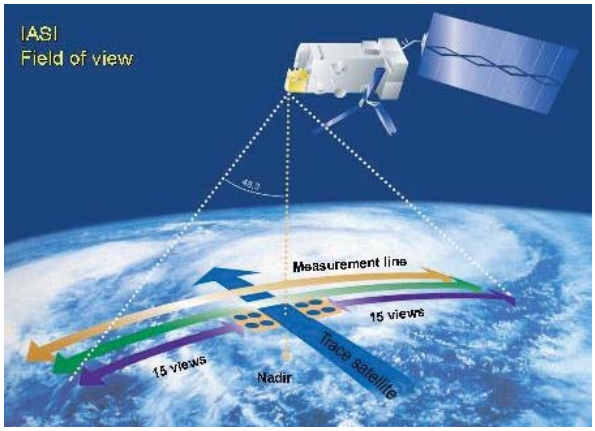

Fig. 1. IASI scanning

A field motion compensation device is integrated in the scan mechanism to ensure view stability during acquisitions so as to avoid contamination of the spectrum resulting from scene radiometric variation.

The IASI instantaneous angular field is conical with a vertex angle of 3.3 degrees. To increase the probability for clear views, it is analyzed by a matrix of 2 x 2 circular independent cells corresponding to a 1.25 degree angle. Their centres are positioned on lines and columns located at ± 0.825 degrees from the instrument optical axis. On the ground, each cell of the analysis matrix corresponds therefore to a circular pixel of 12 km diameter at sub-satellite point.

3. IASI SYSTEM DESCRIPTION

The IASI system is strongly linked to EPS (Eumetsat Polar System) which is developed by EUMETSAT and includes :
(a) The on-board segment which is mainly constituted of the instrument, and its associated on-board software, mounted on the Metop satellite. This segment includes also the software developed for the instrument on-ground acceptance tests.
(b) The operational software is in charge of the instrument scientific data level one processing. This software will be integrated in the EPS core ground segment (see below). The algorithms of the operational software have been validated using the IASI numerical end to end model and the instrument breadboard developed by CNES.
(c) The TEC (Technical Expertise Centre) is in charge of the instrument performance monitoring, the performance anomaly investigation, the development and validation of new algorithms and the maintenance of the on-board and ground software. An overview of the IASI system and the links with EPS is presented in the Fig. 2

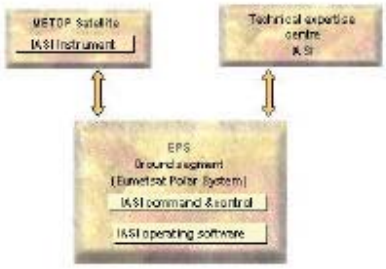

Fig. 2. IASI system overview

4. INSTRUMENT TECHNICAL DESCRIPTION

During technology selections, preference has been given to spectral resolution and radiometric quality, as well as reliability and availability, which are fundamental qualities for an instrument to be operational. The first selection has confirmed the interferometer technique as being preferable to grating spectrometry. In addition, the required quality of radiometric calibration imposes the use of a bilateral interferometer.
The instrument concept is thus based on the Michelson interferometer [3].
The electrical signal from the detector is then digitized before performing a mathematical inverse Fourier transform to restitute the incident radiation spectrum.

The components of IASI, along the light path through the instrument are [4]:
- Scan mirror. Fluid lubricated bearings are used for the step by step scene scanning and the field motion compensation device is based on flexural blade pivot. Life tests were successfully performed on two scan mechanism breadboards.
- Off-axis afocal telescope that transfers the aperture stop onto the scan mirror.
- Michelson interferometer, including a beamsplitter, a compensating plate and two corner cube mirrors : one corner cube moves linearly by ±1 cm within 151 milliseconds, which corresponds to an optical path difference of 2 cm, necessary to obtain the specified spectral resolution. The cube corner reflector is preferable to plane mirror, which would impose dynamic alignment. The very significant number of cycles in the instrument life time (300 millions cycles) and the high reliability required the interferometer mechanism be based on flexible metal guiding blades device.
A 1.54 µm frequency-stabilized laser is injected into the interferometer. Stabilization is achieved by locking the frequency to an acetylene absorption line. The interferometer output of the laser beam is used as a reference to sample the interferogram. This sampling

leads to an important relaxation of the speed stability requirement of the moving reflector.
- A folding mirror directs the recombined beams onto the off-axis focusing mirror, which images the Earth at the entrance of the cold box.
- The cold box (CBS) contains field and aperture stops; the field lens that forms the image of the pupil on the cube corners; the dichroic plates that divide the whole spectrum range into three bands : band 1 is [645 – 1190 cm^{-1}], band 2 is [1190 – 2000 cm^{-1}], band 3 is [2000 – 2760 cm^{-1}] ; objective lenses that image the field stop on the detector unit and the three focal planes, equipped with microlenses, detectors and preamplifiers. The cold box is cooled passively to below 100 K to reduce the instrument background and thermoelectronic detector noise.
Interferograms are digitized with a 16 bits resolution by the acquisition electronics and processed by the digital signal processing subsystem (DPS). The only means to achieve the data rate allocated by Metop to IASI (1.5 Mbits/s) without quality loss was to convert the interferogram (45 Mbits/s) into a complex spectrum, then to perform the inverse Fourier Transform and the radiometric calibration (disappearance of the imaginary part) on-board.
Calibration is achieved by viewing the internal hot blackbody and cold deep space, every eight seconds.
A wide spectral band infrared imager is integrated in IASI to facilitate the processing of partly cloudy regions by a fine analysis of the properties of the clouds present in the IASI field, in conjunction with the AVHRR imager. The IASI imager relies on a microbolometer matrix. It includes a unique 10.5 to 12.5 µm spectral channel (atmospheric window). Its radiometric sensitivity must be higher than 0.5 K at 300 K and it must be calibrated for an accuracy higher than 1K. Its 64 x 64 detector matrix analyses a square field with sides of 3.3 degrees, centred on the sounder optical axis. Each detector of the integrated imager, therefore, sees a square pixel of 0.8 Km sides at sub-satellite point.

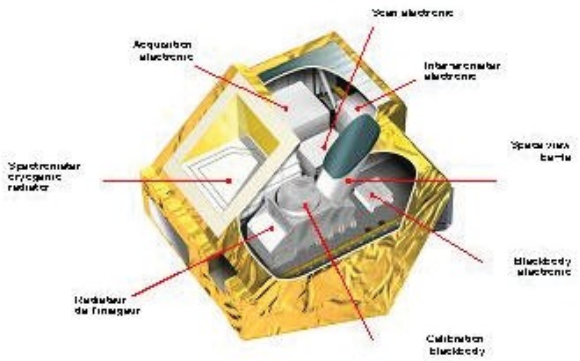

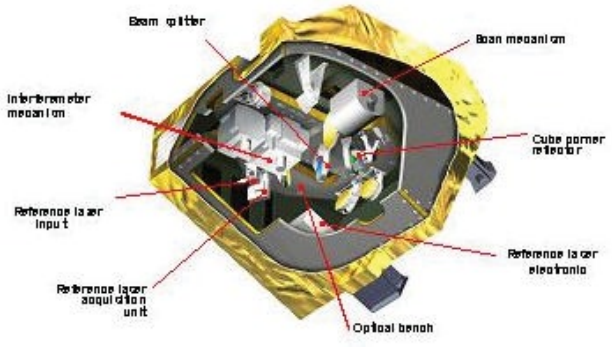

Fig. 3. instrument views

5. IASI PRODUCT DESCRIPTION

The IASI on-board processing system generates calibrated atmospheric spectra from raw interferograms : non-linearities correction, inverse FFT, radiometric calibration. Spectra are downlinked from the satellite to the ground segment, they form level 0 data.

Data are processed on the ground at three levels :
level 1A comprises decoding, spectral calibration, radiometric post-calibration, IASI/AVHRR co-registration, location and dating;
level 1 B consists in resampling the spectra;
level 1 C comprises an apodization function and analysis of AVHRR radiance levels in IASI pixels.
All level 1 data are available for users [5].

6. IASI PFM MEASURED PERFORMANCES

The IASI PFM (Proto Flight Model) instrument optical-vacuum test was performed in June 2003 at ALCATEL premises in Cannes.
Processing of the data has been done in parallel by CNES and ALCATEL. This chapter provides synthesis of the sounder main performances, at instrument level.

6.1 Spectral performances

The spectral specifications can be verified only at the two wave numbers covered by the lasers used in the test facility :

band 1 : CO_2 : 10.59 µm (944.2 cm^{-1})
band 3 : HFDF : 3.77 µm (2655.88 cm^{-1}).

The lasers highlight the field of view and the pupilla of the instrument through an integrating sphere. The lines seen in the output spectra are directly the ILS.

6.1.1 Spectral resolution

The spectral resolution is defined as the full width at half maximum of the ILS. Fig. 4 and 6 show examples of measured ILS :

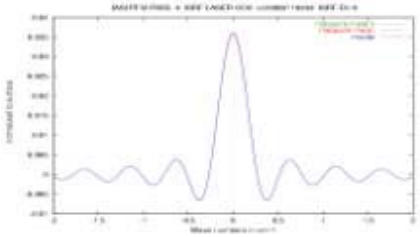

Fig. 4 Example of ILS central part in band 1

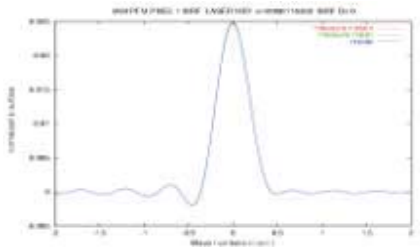

Fig. 5 Example of ILS central part in band 3

The results are synthesized in table 3 :

Table 3. Full Width at Half Maximum of ILS

(cm^{-1})	Pixel 1	Pixel 2	Pixel 3	Pixel 4
Band 1	0.316	0.316	0.319	0.318
Band 3	0.408	0.407	0.465	0.440

We can conclude that the instrument is fully compliant with the resolution specification.

6.1.2 Shape Error Index

The ε tests revealed a parasitic micro-vibration at 380 Hz. Its signature can be seen in Fig. 6 :

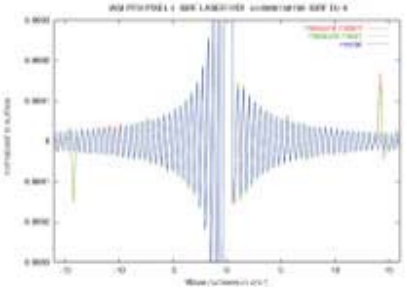

Fig. 6 Zoom of ILS in band 3 (compare to vertical scale in Fig. 5)

The results for ε_1 in table 4 include the effect of the ghost :

Table 4. ε_1 performance of the PFM model

	Pixel 1	Pixel 2	Pixel 3	Pixel 4
Band 1	0.032	0.032	0.026	0.027
Band 3	0.033	0.097	0.045	0.035

But if we exclude the ghost from ε_1 calculation, the instrument is most of the time marginal to the specification in band 1 and always inside the specification in band 3 except for pixel 2.

Despite the ghost, ε_2 performance of the PFM model is within the specification :

Table 5. ε_2 performance of the PFM model

	Pixel 1	Pixel 2	Pixel 3	Pixel 4
Band 1	0.016	0.015	0.011	0.013
Band 3	0.022	0.015	0.015	0.016

The ghost phenomena is analysed on FM2 (Flight Model number 2) in order to make sure that its intensity is limited, because its phase is not stable, therefore there is no way to extract it by a model from the data.

In fact the results presented above are an average of the performances of the nominal instrument and the redundant one. The conclusion on the PFM was that the performance of the nominal instrument meets the specifications of ε, and that the redundant instrument is marginally out of specification, but acceptable.

6.1.3 Spectral stability

The test campaign showed that the instrument has a stability always better than 3.10^{-7} during 480 s, fully compliant with the specification of 10^{-6} during 8 s.

The theoretical spectral shift is defined as the difference between a monochromatic wave number at the entrance of the instrument and the measured one. The maximum shift found during the tests is $1.5.10^{-5}$, fully within the specification.

6.2 Radiometric performances

6.2.1 Result for a scene at 293 K

Fig. 7 shows the noise observed on the internal blackbody target (BBC). The CBS temperature was around 93.4 K.

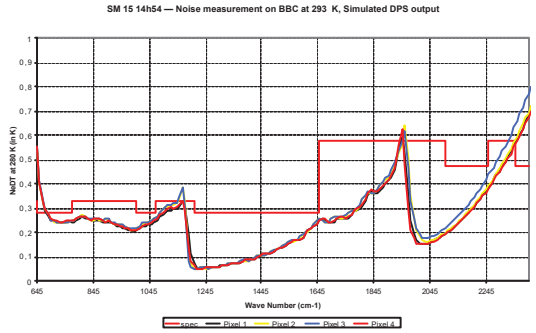

Fig. 7. radiometric noise observed on a target at 293 K (BBC), T_{CBS} = 93,4 K

One sees that compliance with the specification is globally achieved except
- at the beginning of the B1 band (between 645 and 700 cm^{-1}),
- in the B3 band. In this band Pixel 3 is about 15 % more "noisy" than the other pixels.

The radiometric test showed the good quality of the performances. They also are very close to model predictions (less than 10 % differences). We expect even better radiometric performances from new B1 detectors to be delivered soon.

6.2.2 Ice contamination

During the radiometric test, we could note a constant degradation of noise. This was the effect of contamination by ice.

We have tried to estimate what the instrument noise would have been without the ice contamination. The method is based on the knowledge of the absorption coefficient of ice (complex refraction index). First it is proved, through direct observation, that the transmission loss can be modelled with a good accuracy by absorption by a water ice film. Then the thickness of the film is estimated by observing the spectral deformation of the noise curve (mainly in B1 band). This estimation provides as a byproduct the "corrected" noise that would have been obtained without ice contamination.

Fig. 8 shows the "corrected" noise figures for the same measurement sessions as for Fig. 7. An indication of the method validity is given by the good agreement between different curves.

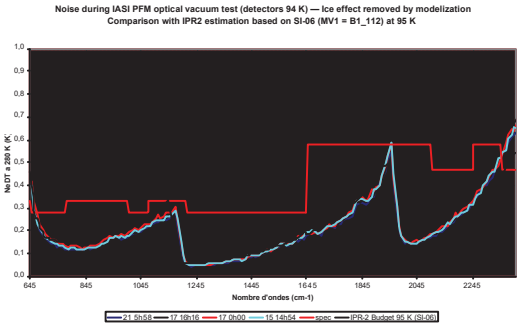

Fig. 8 — Corrected noise : sessions after second de-icing (ice effect removed by model) and comparison with noise budget prediction

The instrument radiometric noise budget predicted from the elementary characteristics measured at equipment level is also reported on the same graph. The noise corrected value is certainly slightly overestimated at the beginning of the B1 band (645-700 cm^{-1}) due to poor knowledge of the absorption coefficient of the ice in this region.

6.2.3 Conclusion for radiometric noise

Preceding section shows that the models used for IASI radiometric noise performance predictions are of good quality.

One more important conclusion to be drawn is that, taking into account the modifications of design which will be implemented on FM2 and other models, for removing ice contamination, the performance of the IASI instrument should be very good in B1 and B2 (largely inside the specifications for wave number larger than 660 cm^{-1} [1]).
Moreover the noise in B1 band, which is very important for the temperature sounding, should even be lower for the next models, according to the performance of the new detectors processed recently.

Compliance with noise specification will be achieved in the B2 and B3 bands too, except in the 2350-2760 cm^{-1} spectral region of the B3 band.

6.3 Calibration absolute accuracy

6.3.1 Measurement method

Radiometric calibration [6] and noise performance assessment are very closely related processes. The difference temperature (between the measure and the reference) are scaled to 280 K according to the instrument specification.

[1] note that the CO_2 branch Q is at 666 cm^{-1}.

6.3.2 Results for a scene at different temperatures

Fig. 9 shows the brightness temperature measured on the external blackbody at about normal incidence on the scan mirror. The CBS temperature is about 93.4 K. The temperature of the HBB (external Hot Black Body, included in the test facility) is 299.65 K

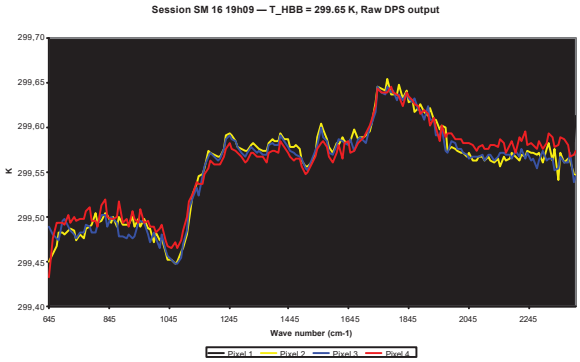

Fig. 9. Brightness temperature observed on a target at 299,65 K (HBB), T_{CBS} = 93,4 K

These curves show that the calibration specification is easily met for a scene at this temperature.

For a scene temperature of 300 K, the error on temperature is bigger than at 293 K but still largely inside the specification : less than 0.2 K.

At 260 K, we could observe that the variations of the measured brightness temperature in the useful IASI band is lower than in the case of 300 K scene and the measure is closer to the reference.

Similarly, the difference of estimated temperature between extreme incidences on the scan mirror (scan positions) is less than 0.2 K.

Other results show that inter-channel calibration is of 0.1 K in the worst case, which is in the specification, albeit the model used for post-calibration is preliminary.

At that stage, one can say that calibration specifications are met, sometimes marginally.

6.4 Point Spread Function

The Instrument Point Spread Function (IPSF), in other words the in field response of the instrument, is specified in chapter 2.4. The uniformity of the IPSF is also specified at ± 5 % within 80 % of the its diameter.

During instrument tests, the four IPSF were measured by scanning the field of view with a spot light at the focus of a collimator. Its size is approximately 1.5 mrd. The three spectral bands for each pixel are acquired. Fig. 10 gives an example of pixel in-field response :

Fig. 10. Tri-dimensional view of pixel 4 IPSF (band 1)

One can see a localized "hole" of sensibility produced by a local default in the field lens. It leads to a slightly out of specification performance for uniformity of pixel 4 in bands 2 and 3. This defect will be corrected when PFM is refurbished. Apart from that, all IPSF features are within the specification.

6.6 Geometric performances (interferometer alignment)

The interferometer alignment requirements are specified in the following table :

Table 6. Internal specification for interferometer alignment (vertical optical bench)

Parameter	Name	Target value
Constant lateral shift along Y axis ...	Y_0	-9 µm ± 14 µm
... along Z axis	Z_0	0 ± 14 µm
Radial linear shift	$\sqrt{Y_1^2 + Z_1^2}$	< 2.5 µm

The lateral shift is defined as the Y and Z components of the $\overrightarrow{C_2C_1'}$ vector, in the C_2 space, with respect to the Y_{CC2} and Z_{CC2} axis (C_i is the summit of corner cube i)

As a summary, the mean retrieval for the interferometer internal alignment (after vibrations tests of the instrument) gives :

Table 7. Internal interferometer alignment for PFM

	Y_0 (µm)	Z_0 (µm)	Y_1 (µm)	Z_1 (µm)
Averaged alignment	10.4	16.5	-4.0	2.1

This is slightly out of specification, but without any impact on contrast, and the good alignment of the CBS compensates the linear shift.

6.7 Contrast evaluation

The coatings of the interferometer optics have non-ideal performances : the anti-reflective coatings have a R factor greater than zero, the beam-splitter is not 50-50, and every coatings and substrates have a certain absorption.

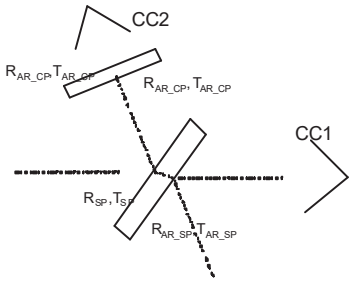

Fig. 11. Radiometric model of the interferometer

These non-ideal performances give rise to a parasitic term that lowers the nominal "apparent" contrast. Other effects impact the contrast, namely the Wave Front Error of interferometer elements, and their alignment.

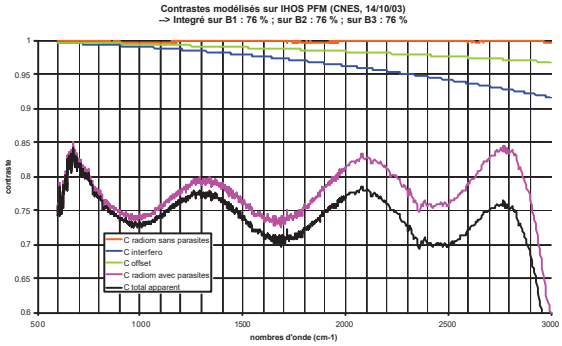

Fig. 12. Model of expected contrast

We can define two types of contrast : a monochromatic contrast, as measured with a laser for instance, and a band-averaged contrast, as measured on a blackbody, integrated within each of the three spectral bands of IASI.

The specified, expected (from our knowledge of the defects of each element) and measured contrasts are given in table 8 :

Table 8. Specified, expected and measured contrasts

Band	Specified	Expected	Measured
@ 3.39 µm	> 59 %	61 %	NA
@ 3.76 µm	> 70 %	73.6 %	74 %
@ 10.6 µm	NA	73.4 %	72 %
Averaged B1	NA	76 %	73.3 %
Averaged B2	NA	76 %	72 %
Averaged B3	NA	76 %	72.6 %

The coherence between measure and model is good enough to be sure that the lose of contrast is due to coating performances only. This difference is 0.014 for laser sessions, and 0.04 at maximum for black body sessions.
Considering the very broad band the coatings have to deal with, it can be considered that their performances, hence the radiometric contrast, are good.

7. CONCLUSION

IASI programme was presented, together with IASI instrument. IASI was fully tested in 2003 for the first time. The test results were presented too.

They show that the first flight model is globally excellent, with some concern about the radiometric degradation due to ice contamination. It shall be noted that design modifications have been implemented to solve this problem on the second and third flight models.

Besides, these models will include new B1 detectors, from which a significant increase of radiometric performance is expected.

Finally the first flight model described in this paper will be refurbished to benefit these improvements.

8. REFERENCES

1. Chalon G., Cayla F.R., Diebel D. 2001, IASI : An advance sounder for operational meteorology, *IAF 2001 conference proceedings*

2. Cayla F. : L'interferomètre IASI. *La météorologie* 8ème série, 32,23-39, 2001

3. Griffiths P.R. and De Haseth J.A. : Fourier transform infrared spectrometry, *John Wiley & Sons, New York*, 1986

4. Simeoni D., Singer C, Chalon G : Infrared Atmospheric Sounding Interferometer, *IAF-96-B.3.P212*, 1996

5. Tournier B., Blumstein D., Cayla F. : IASI Level 0 and 1 processing algorithms description, *International TOVS Science Conference – XII*, 2002

6. Revercomb H.E., Buijs H., Howell H.B., LaPorte D.D., Smith. W.L. and Sromovsky L.A : Radiometric calibration of IR Fourier transform spectrometers : solution to a problem with the High-Resolution Interferometer Sounder, *Applied Optics, Vol. 27, No. 15*, 1988